# Attractive and repulsive contributions of localized excitability inhomogeneities and elimination of spiral waves in excitable media

Guoyong Yuan* and Huan Zhang
*Department of Physics, Hebei Normal University, Shijiazhuang 050024, China and Hebei Advanced Thin Films Laboratory, Shijiazhuang 050024, China*

Aiguo Xu and Guangrui Wang
*Institute of Applied Physics and Computational Mathematics, P.O. Box 8009, Beijing 100088, China*
(Received 30 April 2013; published 26 August 2013)

The attracting and repelling of spiral waves in a two-dimensional excitable medium in the presence of localized excitability inhomogeneities are studied. The choice of two effects depends on the comparison of excitabilities inside and outside the localized obstacle. We inspect the changes in attracting and repelling behaviors with respect to the size of the obstacle and the initial distance between the center of the spiral core and the obstacle. To understand the occurrence of these phenomena, we investigated the small $v$-value areas near the tip and the function of the wave velocity as the excitability parameter $\varepsilon$. Considering the attributes of the attractive obstacle, an eliminating scheme of spiral waves is proposed in which the attractive obstacle is rapidly moved at several fixed times. This method can avoid the high-amplitude and high-frequency stimulus in most conventional methods.

DOI: 10.1103/PhysRevE.88.022920 PACS number(s): 89.75.Kd, 82.40.Ck, 47.54.−r

## I. INTRODUCTION

Spiral waves are typical spatiotemporal patterns in excitable and oscillatory systems [1]. Examples include the cardiac muscle [2], oxidation reaction of CO on Pt catalytic surfaces [3], liquid crystal subjected to an electric or magnetic field [4], slime mould dictyostelium discoideum amobae [5], xenopus oocytes [6], and reacting chemical systems [7]. The characteristics and the dynamics of spiral waves have been studied extensively via theories and experiments.

In fact, many excitable media exhibit inhomogeneities. For example, the heart-muscle tissue is manifestly inhomogeneous, and chemically excitable media may have temperature or other parameter gradients. A large inexcitable obstacle may lead to a local block of a propagating wavefront and the breaking of the wavefront into two separate wavefronts. Subsequent detachment of the two broken wavefronts from the obstacle leads to the formation of two spiral waves [8–11]. When a traveling wave propagates through a narrow isthmus (gap) between inexcitable obstacles, the so-called source-sink mismatch may also lead to spiral wave formation [12,13]. A plane wave propagating through a system with inhomogeneity, introduced by modifying the spatial dependence of the diffusion coefficient in a stochastic manner, may break up in regions with low conductivity and produce numerous spiral waves [14]. Three main scenarios of reentry wave formation were found: unidirectional block, main wave-wavelet collision, and wave breakup during collision, in a region where a conduction velocity gradient occurs. Spiral wave generation in heterogeneous excitable media was discussed in Refs. [15,16].

Recently, the effect of inhomogeneous conditions on spiral dynamics has become a focus of study. Both numerical and experimental studies show that a sufficiently large obstacle can stabilize a rotating wave, preventing the transition to spatiotemporal chaos [17,18]. The suppression of spiral breakup depends sensitively on the position, size, and nature of the inhomogeneity [19,20]. Three-dimensional scroll waves in inhomogeneous media can exhibit twist [21–23], but Jimenez *et al.* have also experimentally observed the pinning of scroll rings to inexcitable heterogeneities, which prevents the collapse of the rings [24]. Recent numerical simulations demonstrated that nonuniform excitable media, consisting of an inner disk part surrounded by an outer ring part with different excitabilities, support the propagation of inwardly rotating spirals [25]. Mechanical deformation in excitable media may also induce spiral breakup [26]. In heterogeneous excitable media with a parameter gradient, normal and anomalous drifts of spiral waves have been observed [27,28]. Spiral waves propagating in randomly distributed obstacles were also extensively considered [29–32]. The number of inexcitable cells or obstacles influences the conduction velocity of the plane wave and the effective diffusion coefficient in the eikonal curvature equation, as well as the breakup of spiral waves [29,30]. In the two-state medium of the light-sensitive Belousov-Zhabotinsky system, different percolation thresholds for propagation were observed by controlling the number of sites with a given illumination [31]. When the inhomogeneity of the anisotropy level is modeled by adding Gaussian noise to diffusion coefficients corresponding to lateral coupling of the cells, different noise intensities induce different dynamical behaviors of the spiral wave [32].

When spiral waves occur in biological excitable media such as the heart, they are associated with the breakdown of its normal rhythmic pumping action. Controlling these spiral waves using low-amplitude external perturbation is not only a problem of fundamental interest in the study of the dynamics of excitations in active media, but it also has significant implications for the clinical treatment of cardiac arrhythmias [33–40]. In a finite medium with no-flux boundaries, periodic high-frequency stimulation (pacing) from a localized region in the excitable medium can generate wave trains that interact

*g-y-y1975@sohu.com

 

with the spiral wave. If the frequency of external stimulation is higher than the rotation frequency of the spiral wave, the spiral core is eventually driven to the boundary and thereby eliminated from the system [33–36]. The above argument can account for the removal of spirals in a homogeneous medium. It is well known that spiral waves are often stabilized by anchoring (pinning) to a local heterogeneity, and that such pinned waves are rather difficult to eliminate. A few recent studies have suggested that pacing-induced unpinning and pacing-induced elimination of spiral waves may occur in inhomogeneous media with a large inexcitable obstacle [41–47].

In most of the previous studies, the selected obstacles do not support the propagation of excited waves. In numerical simulations, the obstacles are often treated as no-flux or Dirichlet boundary conditions [48,49]. In fact, the effects of the spiral waves depend on the types of heterogeneities. In this paper, we will study the interaction of spiral waves with a local inhomogeneous domain consisting of excited units with a different excitability. Examples of obstacles with different excitability include scar tissue or ionic heterogeneities. This paper is organized as follows. In Sec. II we describe the mathematical model used in this study. Sections III and IV contain the numerical results of attractive and repulsive attributes of the localized inhomogeneities. In Sec. V we provide an interpretation for these attributes of the obstacle, and in Sec. VI an eliminating scheme of spiral waves is suggested. Section VII contains the conclusion and a discussion of the results.

## II. THE MODEL WITH A LOCALIZED INHOMOGENEITY

We consider the FizHugh-Nagumo (FHN) model [50,51], which is a set of two-variable "reaction-diffusion" equations that captures the key features of excitable media. This model can reproduce many qualitative characteristics of electrical impulses along nerve and cardiac fibers, such as the existence of an excitation threshold, relative and absolute refractory periods, and the generation of pulse trains under the action of external currents. The model is described as follows:

$$\frac{\partial u}{\partial t} = \frac{1}{\varepsilon}[-v - u(u-a)(u-1)] + \nabla^2 u, \tag{1}$$

$$\frac{\partial v}{\partial t} = -\gamma v + \beta u - \delta, \tag{2}$$

where $u$ is a voltagelike variable and $v$ is a recovery variable. In this model, $a$ represents the threshold for excitation, $\varepsilon$ represents excitability, and $\gamma$, $\beta$, and $\delta$ are parameters controlling the rest state and the dynamics. In this paper, we set the parameters $a = 0.03$, $\gamma = 1.0$, $\delta = 0.0$, and $\beta = 2.0$. In numerical simulations, the system (1)–(2) is integrated by the operator-splitting method with the time step $\Delta t = 0.005$, the lattice size $h = 0.1$, and a $200 \times 200$ array. The no-flux boundary condition is chosen.

The parameter $\varepsilon$ is a measure of the excitability. An increase in $\varepsilon$ implies a reduction in the excitability of the medium. A sequence of spiral states can be obtained as a function of the parameter $\varepsilon$ in the homogeneous media with the above fixed other parameters. When $\varepsilon > 0.004\,65$, the rigidly rotating wave (RW) is observed as a stable spiral state, and its tip traces a circumference. For $\varepsilon < 0.004\,65$, modulating rotating waves (MRWs) appear as a general class of dynamic states in the medium and two-frequency quasiperiodic states which are periodic when viewed in an appropriately rotating reference frame. The meandering tip trajectory of MRWs resembles a hypocycloid of radius $R_{\mathrm{MRW}}$, and increasing the value of $\varepsilon$ increases the radius $R_{\mathrm{MRW}}$. When $\varepsilon = 0.004\,65$, the value of $R_{\mathrm{MRW}}$ tends to infinity, and we obtain a cycloid trajectory (hypocycloid with $R_{\mathrm{MRW}} \to \infty$). The corresponding spiral state is referred to as the modulated traveling wave (MTV).

Initially, a spiral wave is generated by cutting off a traveling pulse in the homogeneous system with an excitability parameter $\varepsilon = \varepsilon_{\mathrm{ini}}$. To study the spiral wave interacting with localized excitable inhomogeneities, after the formation of the spiral wave, a localized inhomogeneity is implemented by introducing a circular region of radius $R_{\mathrm{obs}}$ centered at the location $(x_{\mathrm{obs}}, y_{\mathrm{obs}})$, inside which the excitability parameter is different from $\varepsilon_{\mathrm{ini}}$ and has a value of $\varepsilon = \varepsilon_{\mathrm{obs}}$. The excitable obstacles may be scar tissue or ionic heterogeneities in cardiac tissue.

## III. ATTRACTIVE ATTRIBUTES OF LOCALIZED INHOMOGENEITIES

Numerical results demonstrate that the effects of localized excitability inhomogeneities on spiral dynamics depend sensitively on the excitability parameters inside and outside the circular obstacle. A spiral wave is initiated in the homogeneous medium with an excitability parameter $\varepsilon_{\mathrm{ini}} = 0.003$, and its core is centered at $(x_{\mathrm{sp}}^{\mathrm{core}}, y_{\mathrm{sp}}^{\mathrm{core}}) \approx (103, 100)$ by suitably selecting the cutoff time. After full development of the state, a circular obstacle, with a radius $R_{\mathrm{obs}} = 5$, is placed at (115,100) near the spiral core. With this setup, it is described in Fig. 1 how the excitability inside the obstacle affects the spiral dynamics. Two characteristic behaviors are clearly observed: For $\varepsilon_{\mathrm{obs}} < \varepsilon_{\mathrm{ini}}$, repulsion occurs [see Fig. 1(a)], while for $\varepsilon_{\mathrm{obs}} > \varepsilon_{\mathrm{ini}}$, the spiral tip may be attracted to the obstacle [see Figs. 1(b) and 1(c)]. In the section, we consider the attractive case, namely the case of $\varepsilon_{\mathrm{obs}} > \varepsilon_{\mathrm{ini}}$.

The bottom panels of Fig. 1 exhibit that spiral dynamics change with the distance $d$ between the initial spiral wave core and the center of the obstacle by varying $x_{\mathrm{obs}}$, where $y_{\mathrm{obs}} = 100$ is fixed. An attraction occurs for small values of $d$, and increasing $d$ can lead to a decrease in attractive velocity. When $d$ is increased beyond a critical value, the attractive action disappears, and the initial tip trajectory is almost not influenced by the obstacle. On the other hand, the size of the obstacle is also an important factor in determining whether or not the attraction takes place and how fast the initial tip is attracted. For a suitable $d$, the spiral core does not drift when $R_{\mathrm{obs}}$ is very small. As $R_{\mathrm{obs}}$ is increased beyond a critical value, the attractive action appears.

To describe how fast the initial core enters the obstacle, we define $T_{\mathrm{attr}}$ as the spent time from the appearance of the obstacle to the onset of the initial tip just entering the obstacle. It is obvious that a fast attracting behavior has a small $T_{\mathrm{attr}}$. The quantitative descriptions for the change of $T_{\mathrm{attr}}$ with $x_{\mathrm{obs}}$, $R_{\mathrm{obs}}$, and $\varepsilon_{\mathrm{obs}}$ are shown in Fig. 2. When $x_{\mathrm{obs}}$ is not very large, $T_{\mathrm{attr}}$ is an increased function of $x_{\mathrm{obs}}$, and the function

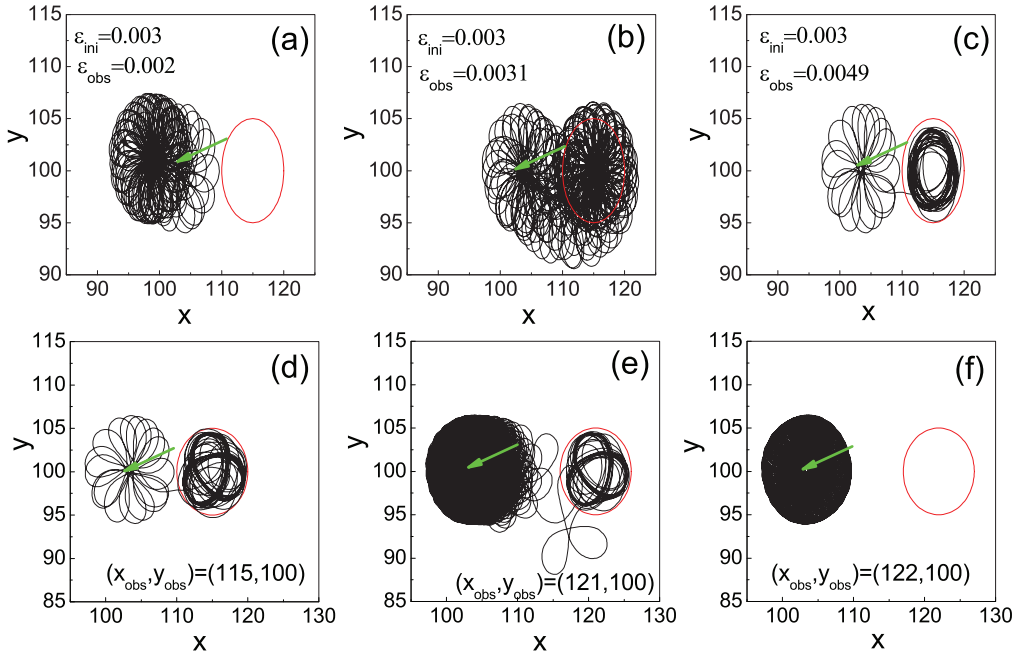


FIG. 1. (Color online) The effects of an excitability obstacle on the spiral tip motion for different values of $\varepsilon_{\text{obs}}$ (top panels) and $d$ (bottom panels), where the initial spiral core is out of the obstacle. Top panels: (a) $\varepsilon_{\text{obs}} = 0.002$, (b) $\varepsilon_{\text{obs}} = 0.0031$, and (c) $\varepsilon_{\text{obs}} = 0.0045$ for a fixed location $(x_{\text{obs}}, y_{\text{obs}}) = (115,100)$. Bottom panels: (d) $x_{\text{obs}} = 115$, (e) $x_{\text{obs}} = 121$, and (f) $x_{\text{obs}} = 122$ for a fixed $\varepsilon_{\text{obs}} = 0.0045$. Here $\varepsilon_{\text{ini}} = 0.003$, $R_{\text{obs}} = 5$, and $y_{\text{obs}} = 100$.

has an approximate exponent [see Fig. 2(a)]. For $x_{\text{obs}}$ beyond a critical value, the attractive motion is terminated. The speed of attractive motion depends also on $R_{\text{obs}}$. As $R_{\text{obs}}$ is increased, $T_{\text{attr}}$ is gradually reduced [see Fig. 2(b)], namely the obstacle with a large $R_{\text{obs}}$ leads to a fast attractive motion. Figures 2(c) and 2(d) depict the relations between $T_{\text{attr}}$ and $\varepsilon_{\text{obs}}$ for two cases of $R_{\text{obs}} = 5$ and 12 under $\varepsilon_{\text{ini}} = 0.003$, and they are two decreasing functions with an approximately exponential form.

The attractive behavior is also reflected in another case, where the obstacle contains the spiral core [see Figs. 3(a)–3(c)]. From Fig. 3(a), we can observe that the tip trajectory will be compressed in the obstacle when it is incompletely

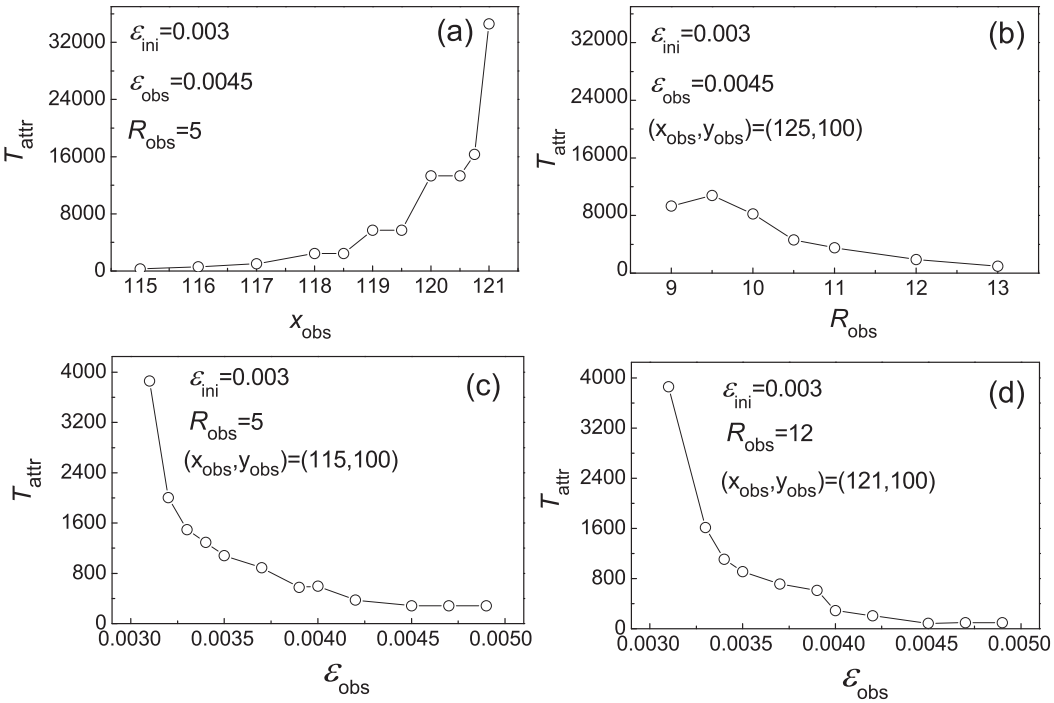


FIG. 2. Quantitative descriptions for the change of $T_{\text{attr}}$ with $x_{\text{obs}}$ (a), $R_{\text{obs}}$ (b), and $\varepsilon_{\text{obs}}$ (c) and (d) when the initial spiral core is out of the obstacle. The corresponding parameters are descried in their own subplots.

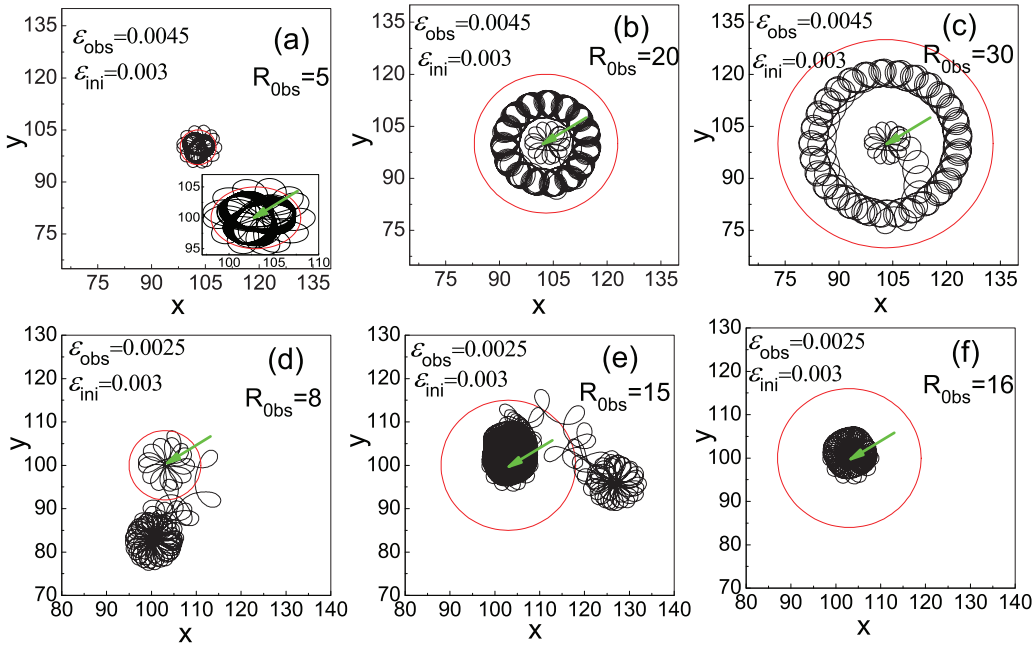


FIG. 3. (Color online) Attractive and repulsive cases of the obstacle when the initial spiral core is in the obstacle. Top panels: attractive illustration for $\varepsilon_{obs} > \varepsilon_{ini}$ and its change with $R_{obs}$. Bottom panels: repulsive illustration for $\varepsilon_{obs} < \varepsilon_{ini}$ and its change with $R_{obs}$. Here $(x_{obs}, y_{obs}) = (103, 100)$, and the other parameters are descried in their own subplots. The inset in the first subplot shows an enlarged version.

contained. If the initial tip trajectory is completely contained, the final trajectory is still in the obstacle and its size is a linearly increasing function of $R_{obs}$, which is shown in Figs. 4(a) and 4(b). The increasing relation will be terminated when $R_{obs}$ is beyond a critical value. In this case, the final trajectory agrees with that of the spiral wave in the uniform medium with an excitability parameter $\varepsilon_{obs}$.

## IV. REPULSIVE ATTRIBUTES OF LOCALIZED INHOMOGENEITIES

Figure 1(a) illustrates the repulsive attributes of the obstacle with an excitability parameter $\varepsilon_{obs} < \varepsilon_{ini}$. Further study shows that the action is short-distance, i.e., it works for a small $d$. In Fig. 5, a rigid rotating spiral is initially generated in the homogeneous medium with an excitability parameter $\varepsilon_{ini} = 0.0049$, and its core is at $(75, 102)$. In the top panels, the obstacle, with an excitability $\varepsilon = 0.001$ and a radius $R_{obs} = 5$, is placed along $y_{obs} = 102$. For small $d$, it is observed that the spiral core is repelled, but the repulsion will be terminated after the spiral core moves a short distance away from the obstacle [see Figs. 5(a) and 5(b)]. After the repulsive action is terminated, the instantaneous rotating core of the spiral wave moves along a limit circle centered at $(x_{obs}, y_{obs})$, while for larger $d$, the repulsive action is out of work. In contrast, the spiral core is attracted to the limit circle [see Fig. 5(c)], and the attractive case is different from the one for $\varepsilon_{obs} > \varepsilon_{ini}$ because the spiral core is attracted into the obstacle in the latter case.

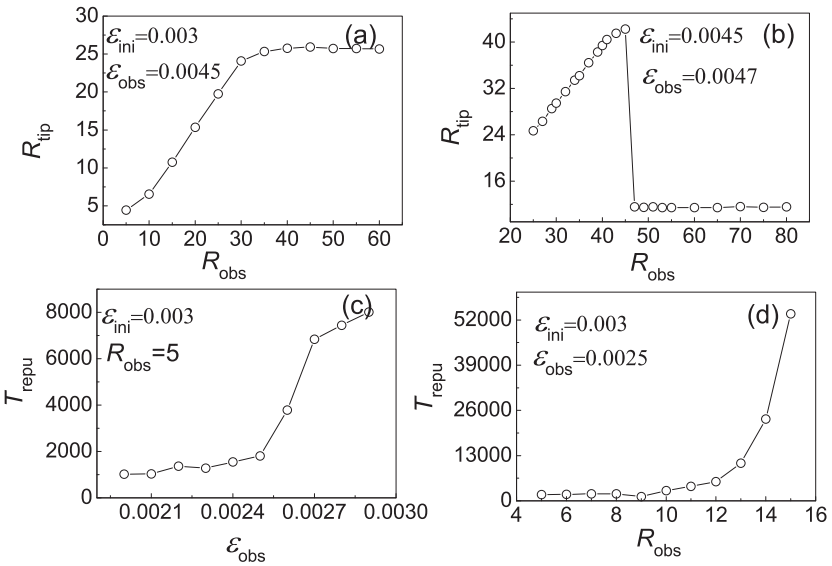


FIG. 4. Four quantitative descriptions for attractive and repulsive cases when the initial spiral core is in the obstacle. (a) $R_{tip}$ as a function of $R_{obs}$ in the attractive case, where values of the other parameters are the same as in Fig. 3(a); (b) $R_{tip}$ vs $R_{obs}$ in the attractive case, where $(x_{obs}, y_{obs}) = (83, 122)$; (c) $T_{repu}$ as a function of $\varepsilon_{obs}$ in the repulsive case, where $(x_{obs}, y_{obs}) = (103, 100)$; (d) $T_{repu}$ vs $R_{obs}$ in the repulsive case, where $(x_{obs}, y_{obs}) = (103, 100)$.

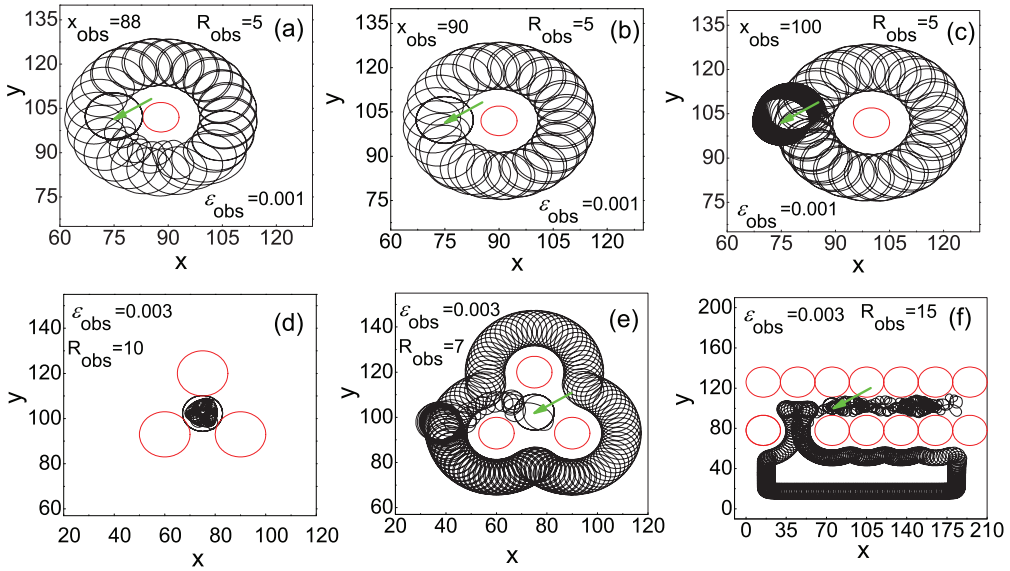


FIG. 5. (Color online) Illustration of a repulsive attribute when the initial spiral core is out of the obstacle. Top panels: illustration for the repulsive action and its short-distance nature of the repulsive action in the single-obstacle case, where three different values of $x_{\rm obs}$ are considered. Bottom panels: repulsive action in the multiple-obstacles case. For all subplots, $\varepsilon_{\rm ini} = 0.0049$, and the other parameters are marked in their own subplots.

The bottom panels exhibit the repulsive attribute of multiple localized obstacles. In Figs. 5(d) and 5(e), three obstacles are symmetrically located to form an equilateral triangle, and its center agrees approximately with the initial spiral core. When $R_{\rm obs}$ is larger, i.e., the gap between the two obstacles is smaller, the initial tip trajectory will be compressed [see Fig. 5(d)], while for a smaller $R_{\rm obs}$, the spiral core can be squirted out along one gap, after which it moves along a triangular closed path around three obstacles [see Fig. 5(e)]. In Fig. 5(f), many obstacles are regularly arranged along two lines, which are parallel to each other, and the lack of an obstacle is designed in the bottom line. The initial spiral core lies between two arrays of obstacles, and it is squirted out along the lacking position. The crowded core will enter the space between two lines again through traveling along the boundary and the bottom line, and then it will be squirted out once again.

The repulsive attribute is further illustrated for another case, where the initial spiral core is in the obstacle [see Figs. 3(d)–3(f)]. In this case, the spiral core will be driven to the outside of the obstacle, and the speed of the driven motion depends on the size of the obstacle. When $R_{\rm obs}$ is beyond a critical value, the outward movement is terminated [see Fig. 3(f)], and the final tip trajectory agrees with that of the spiral wave in the uniform medium with an excitability parameter $\varepsilon_{\rm obs}$. To describe the repulsive effect quantitatively, we define $T_{\rm repu}$ as the spent time from the appearance of the obstacle to the onset of the tip just moving out of the obstacle. The functions $T_{\rm repu}(\varepsilon_{\rm obs})$ and $T_{\rm repu}(R_{\rm obs})$ are exhibited in Figs. 4(c) and 4(d). They reveal the changes with an exponential form.

## V. MECHANISM OF REPULSIVE AND ATTRACTIVE MOTION

Figure 6 shows the tip trajectory during the drawn motion of a meandering spiral wave after switching on an attracting obstacle, and the comparison with the corresponding tip trajectory in the absence of the obstacle. To clearly show the details, the attracted motion is divided into four parts with the same time intervals, which are respectively exhibited in four panels. For a meandering spiral wave, the curve obtained by tracing the motion of the spiral tip describes a flower pattern, where similar loops appear periodically. The loops are called as petals, on which the tip path has a large curvature. Between two adjacent petals, there exists a section of flat path with a very small curvature. In the presence of the attracting obstacle, when the excited state passes through it, the tip motion has a small change, which depends on the distance between the tip position and the obstacle one. The accumulation of small changes may induce a large change, and the tip is attracted to the obstacle, which is shown in Fig. 6(c). After the tip enters the obstacle, its tip path has a large difference with the original tip path [see Fig. 6(d)].

The mechanism of the attractive motion can be understood by studying the areas with small $v$ values (SV areas) near the spiral tip (the SV areas are illustrated by blue in Fig. 7). From the kinetic analysis of the excitable system, it is known that the propagation is quicker on those parts of the $u$ spiral behind the SV areas. By analyzing the size and placing of the SV areas, we can explain the tip motion of the spiral wave. In the second and fourth rows of Fig. 7, panels (a′)–(l′) show snapshots of SV areas and contours of $u$ spirals near the tip for 12 different times in the absence of the obstacle. The corresponding tip location at each time is shown by cyan points and cyan numbers 1–12 in Fig. 6(c), where the blue curve describes the tip motion within a time interval of 140 time steps from $t = 300$ to 440 in the absence of the obstacle. When the tip reaches the cyan point "1," the SV areas do not appear in the normal front of the partial wavefront close to the tip [see Fig. 7(a′)], and this means that the propagation of the front segment is terminated or slowed down. The corresponding wave back segment still propagates along the original direction, and it indicates that the tip will be retracted, rather than rolling forward. As the

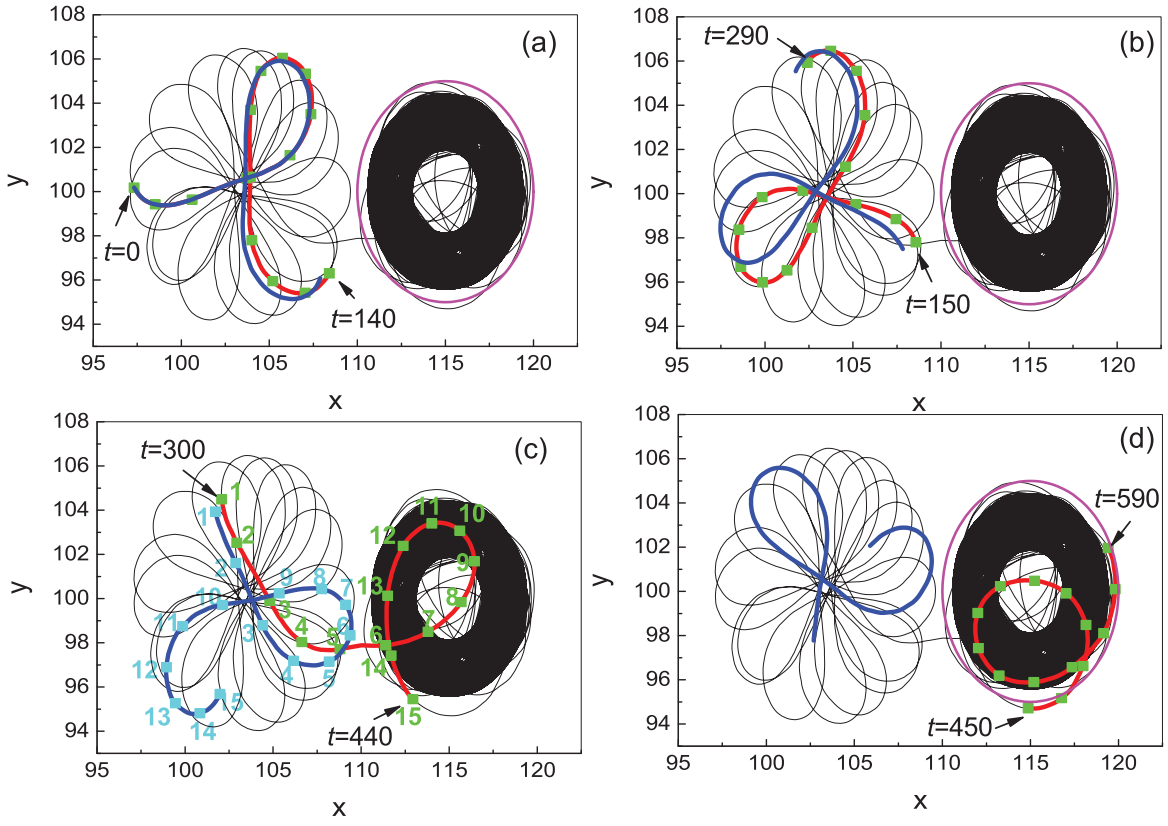


FIG. 6. (Color online) Illustration of the tip trajectory for the attracting phenomenon, and comparison with the tip trajectory in the absence of the obstacle. The black curve describes a whole trajectory in the attracted process, which includes a small part of the tip path before $t = 0$ ($t = 0$ corresponds to the moment of the onset of the obstacle). (a) Comparison of tip trajectories in the presence of the obstacle (red line) and in the absence of it (blue line), within a time interval from $t = 0$ to 140; (b) within a time interval from $t = 150$ to 290; (c) within a time interval from $t = 300$ to 440; and (d) within a time interval from $t = 450$ to 590. The time interval, between two adjacent square scatters in each curve, is 10 time steps. Here, the parameters are as follows: $\varepsilon_{\text{ini}} = 0.003$, $\varepsilon_{\text{obs}} = 0.0045$, $R_{\text{obs}} = 5$, and $(x_{\text{obs}}, y_{\text{obs}}) = (115, 100)$.

tip moves from point "1" to point "3," the distance between the partial wavefront close to the tip and the wave back in the normal front of them will become large, which can lead to the gradual extension of the SV areas toward the tip along the the spiral front [see Figs. 7(a′)–7(c′)]. Therefore, the path of this movement is very flat or straight. After the tip arrives at point "3," the SV areas begin to appear in the normal front of the tip [shown in Figs. 7(c′)–7(f′)], which causes the tip to roll forward and move along a petal path. With the fast propagation of the tip part, the distance from the tip to the forward wave back begins to become small, and the SV areas in the normal front of the tip will disappear [see Figs. 7(g′)–7(l′)]. The tip moves along a flat path again.

Now, we analyze the effects of the obstacle by comparing the SW areas in the presence of the obstacle with those in the absence of the obstacle within the same time interval. In the first and third rows of Fig. 7, panels (a)–(l) show snapshots of SV areas and contours of $u$ spirals near the tip for 12 different times in the presence the obstacle. The corresponding tip location at each time is shown by green points and marked numbers 1–12 in Fig. 6(c), where the red curve describes the tip motion within a time interval of 140 time steps from $t =$ 300 to 440 in the present of the obstacle. At $t = 300$ (the tip reaches the position "1"), a part of the excited arm just passes through the obstacle. It can be proven by theoretical analysis and numerical results that the decreasing velocity of excitable waves behaves as a function of $\varepsilon$. Therefore, the propagation of the excited part is slowed down due to $\varepsilon_{\text{obs}} > \varepsilon_{\text{ini}}$, which is illustrated by observing the domain indicated by an arrow in Fig. 7(a). It is followed by reducing the distance between the tip and the excited part. As a result of this change, the appearance of the SV areas is delayed, which can be seen by a comparison of Figs. 7(c) and 7(c′). The sharply turning movement is postponed and flattened, and what follows then is that the tip enters the obstacle directionally. In the obstacle, the propagation of the tip part is slowed down. While the propagation velocity of the excited part in the normal front of the tip part is not reduced, there exist large SV areas around the tip [see Figs. 7(g)–7(l)]. This results in the turning movement of the tip and the lack of the flat movement, and the tip is bound in the obstacle.

The attractive effects are also understood by the eikonal equation ($c_n = c_0 - D\kappa$), where the front velocity in its normal direction depends on its local curvature. After a part of the excited front passes through the obstacle, its curvature will become small. What follows then is that two high-curvature junction sections appear in the front, one of which moves toward the tip along the front curve with the continued evolution of the spiral wave due to the requirement of the eikonal equation. For the repulsive cases, the propagation

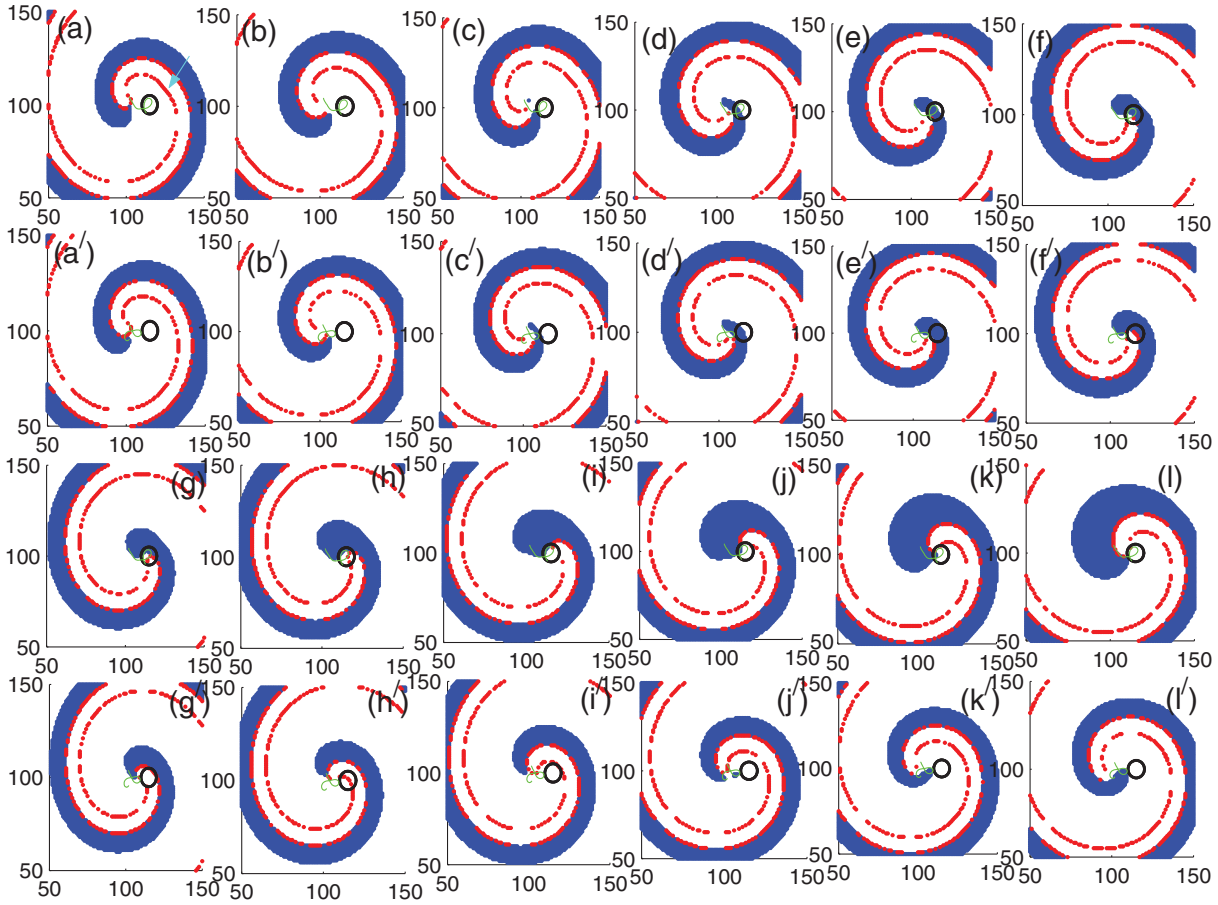


FIG. 7. (Color online) Snapshots of SV areas (marked in blue) and contours of $u$ spirals (marked in red) near the tip for 12 different times in the presence of the obstacle (first and third panels) and in the absence of the obstacle (second and fourth panels). $t = 300$ in (a) and (a′), $t = 310$ in (b) and (b′), $t = 320$ in (c) and (c′), $t = 330$ in (d) and (d′), $t = 340$ in (e) and (e′), $t = 350$ in (f) and (f′), $t = 360$ in (g) and (g′), $t = 370$ in (h) and (h′), $t = 380$ in (i) and (i′), $t = 390$ in (j) and (j′), $t = 400$ in (k) and (k′), $t = 410$ in (l) and (l′). The back circle describes the localized obstacle. The parameters are the same as in Fig. 6.

of the excited part, passing through the repulsive obstacle, is speeded up due to $\varepsilon_{\text{obs}} < \varepsilon_{\text{ini}}$. Considering this point, the repulsive behavior can be explained by studying the SV areas near the tip or the changing of the front curvature.

## VI. ELIMINATING SCHEME OF SPIRAL WAVES BASED ON ATTRACTIVE MOTION

Many of the studies on eliminating spiral waves are inspired by the relevance of this topic to the functioning of the heart under normal and pathological conditions. Spiral waves are believed to be responsible for cardiac tachyarrhythmias and are precursors of ventricular fibrillation. Thus, the development of methods to terminate spiral waves would be an important contribution to this field of medicine. In the present study, we shall provide a technique that is based on the attractive contribution of a moving excitability obstacle with $\varepsilon_{\text{obs}} > \varepsilon_{\text{ini}}$. In this scheme, the center of the obstacle moves abruptly a distance $d$ toward the boundary at scheduled time intervals. We define the time interval between two adjacent movements as $T_{\text{moving}}$, and a sufficiently large $T_{\text{moving}}$ is necessary for eliminating spiral waves, where the spiral core is successively attached to the obstacle and moves toward the boundary together with the moving obstacle.

Figures 8(a)–8(e) give an illustration of this eliminating scheme. A spiral wave is first generated in the uniform medium with an excitability parameter $\varepsilon_{\text{ini}} = 0.003$ and its core lies at $(x_{\text{sp}}^{\text{core}}, y_{\text{sp}}^{\text{core}}) \approx (103, 100)$. Then an excitability obstacle [marked by circle "1" in Fig. 8(e)], with a radius of $R_{\text{obs}} = 5$, is simulated at $(x_{\text{obs}}, y_{\text{obs}}) = (115, 100)$, and the spiral core will be rapidly attracted to this obstacle. After $T_{\text{moving}} = 3500$, the obstacle shifts suddenly a distance $d = 12$ toward the right boundary along $y = 100$, i.e., the inhomogeneous excitability appears suddenly in the "2" circular region, and the spiral core will be attracted to the circular region [see Fig. 8(e)]. The two processes of obstacle motion and core attraction take place periodically in turn before the moving obstacle reaches the right boundary. After the obstacle is abruptly moved seven times, it arrives at the boundaries and appears in the semicircular region marked by "8," and a part of the obstacle has stepped out of the medium. The spiral tip is attracted by the semicircular obstacle, and disappears on the boundary [see Fig. 8(d)]. Due to the absence of the tip, the excitable wave will soon disappear.

The value of $d$ required for eliminating the spiral wave must be small enough to ensure the occurrence of attractive

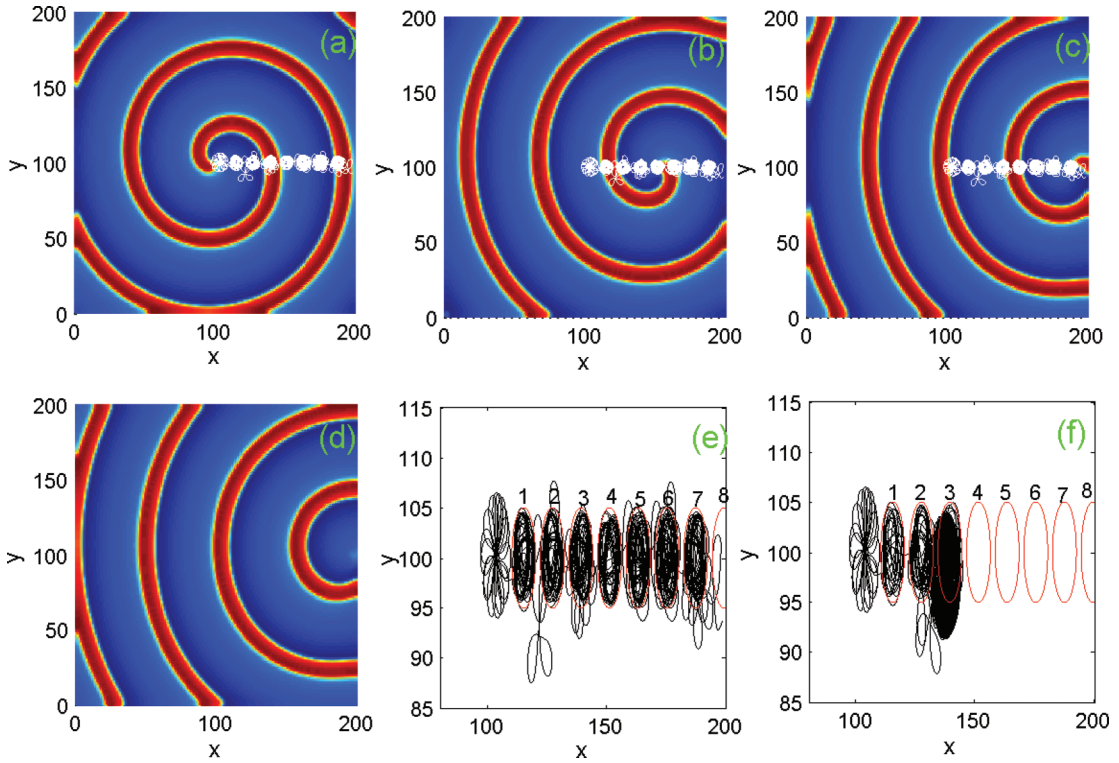


FIG. 8. (Color online) Snapshots and tip trajectories of spiral waves driven by the moving attractive obstacle, where $\varepsilon_{\text{ini}} = 0.003$, $\varepsilon_{\text{obs}} = 0.0045$, $R_{\text{obs}} = 5$, and $d = 12$. An example of successfully eliminating spiral waves is illustrated in panels (a)–(e), where $T_{\text{moving}} = 3500$. (a) Spiral snapshot at $t = 0$ which corresponds to the onset of the moving obstacle. (b) Spiral snapshot at $t = 6610$. (c) Spiral snapshot at $t = 12\,525$. (d) Spiral snapshot at $t = 25\,400$. (e) The corresponding tip trajectory and the position of the moving obstacle for different times. Failure of the elimination is shown in (f), where $T_{\text{moving}} = 1800$.

behaviors. On the other hand, a large enough $T_{\text{moving}}$ is also necessary. For a large $T_{\text{moving}}$, before the obstacle moves again, the stable spiral state can be formed, which ensures the success of the next attractive behavior. For a small $T_{\text{moving}}$, the spiral core is pulled toward the boundary, but it cannot get to the boundary. Figure 8(f) depicts the tip trajectory for the case of $T_{\text{moving}} = 1800$, where the spiral core is pulled only to the position of the "3" circular region.

## VII. CONCLUSION AND DISCUSSION

The existence of localized inhomogeneities in excitable media, such as cardiac tissue, is generally associated with the formation of spiral waves and the changing of spiral wave reentries. To investigate the formation of spiral waves in cardiac tissue, the interactions of traveling or target waves of excitation and these regions are extensively analyzed, where the inhomogeneous regions are idealized as inexcitable and nonconducting. In fact, most excitable media have regions of reduced and enhanced excitability, which can be induced by scar tissue and ionic heterogeneities in the heart. Here, we have examined the effects of those excitability obstacles on fully developed spiral waves. Depending on the excitability of the localized inhomogeneity, our results prove the existence of two different interactions. The reduction of excitability in the obstacle causes an attraction phenomenon of the spiral tips, provided their locations are close enough to each other. On the other hand, the enhanced excitability has a repelling effect. When the initial spiral core is very close to the obstacle, it is repelled and moves a distance away. After moving the distance, the following motion depends on the type of spiral wave. For RW, the tip rolls along a circular limit cycle, centered at the center of the obstacle, while for MRW, the tip meanders in a small region. These behaviors can be understood by studying the changing of SV areas in front of the wavefront, because these SV areas determine the propagation of the front.

We have also proposed a control scheme of spiral waves, which is designed on the basis of the attraction phenomenon in the presence of the excitability-reduced obstacle. In the scheme, the obstacle is initially located close to the original spiral tip, and it will be shifted a small distance after completing the attracting behavior. The practice of repetition is continued until the disappearance of the spiral wave. This method can avoid the high-amplitude and high-frequency stimulus in the traditional methods.

## ACKNOWLEDGMENTS

This work is supported by the National Natural Science Foundation of China (under Grants No. 11005030 and No. 11075021), the Natural Science Foundation of Hebei Province, China (under Grant No. A2013205147), the Scientific Research Foundation of the Education Department of Hebei Province, China (under Grant No. 2009135), and the Science Foundation of Hebei Normal University.

[1] M. C. Cross and P. C. Hohenberg, Rev. Mod. Phys. **65**, 851 (1993).
[2] M. Courtemanche, Chaos **6**, 579 (1996).
[3] S. Nettesheim, A. V. Oertzen, H. H. Rotermund, and G. Ertl, J. Chem. Phys. **98**, 9977 (1993).
[4] T. Frisch, S. Rica, P. Coullet, and J. M. Gilli, Phys. Rev. Lett. **72**, 1471 (1994).
[5] C. van Oss, A. V. Panfilov, P. Hogeweg, F. Siegert, and C. J. Weijer, J. Theor. Biol. **181**, 203 (1996).
[6] J. Lechleiter, S. Girard, E. Peralta, and D. Clapham, Science **252**, 123 (1991).
[7] A. T. Winfree and S. H. Strogatz, Physica D **8**, 35 (1983).
[8] A. V. Panfilov and J. P. Keener, J. Theor. Biol. **163**, 439 (1993).
[9] K. Agladze, J. P. Keener, S. C. Müller, and A. Panfilov, Science **264**, 1746 (1994).
[10] C. Cabo, A. M. Pertsov, J. M. Davidenko, W. T. Baxter, R. A. Gray, and J. Jalife, Biophys. J. **70**, 1105 (1996).
[11] G. Fernández-García, M. Gómez-Gesteira, A. P. Muñuzuri, V. Pérez-Muñuzuri, and V. Pérez-Villar, Eur. J. Phys. **15**, 221 (1994).
[12] C. Cabo, A. M. Pertsov, W. T. Baxter, J. M. Davidenko, R. A. Gray, and J. Jalife, Circ. Res. **75**, 1014 (1994).
[13] V. G. Fast and A. G. Kléber, Cardiovasc. Res. **33**, 258 (1997).
[14] P. Kuklik and J. J. Zebrowski, Chaos **15**, 033301 (2005).
[15] G. Bub, A. Shrier, and L. Glass, Phys. Rev. Lett. **88**, 058101 (2002).
[16] J. Maselko and K. Showalter, Physica D **49**, 21 (1991).
[17] F. Xie, Z. Qu, and A. Garfinkel, Phys. Rev. E **58**, 6355 (1998).
[18] M. Valderrábano, Y. H. Kim, M. Yashima, T. J. Wu, H. S. Karagueuzian, and P. S. Chen, J. Am. Coll. Cardiol. **36**, 2000 (2000).
[19] T. K. Shajahan, S. Sinha, and R. Pandit, Phys. Rev. E **75**, 011929 (2007).
[20] T. K. Shajahan, A. R. Nayak, and R. Pandit, PLoS ONE **4**, e4738 (2009).
[21] A. S. Mikhailov, A. V. Panfilov, and A. N. Rudenko, Phys. Lett. A **109**, 246 (1985).
[22] V. G. Fast and A. M. Pertsov, Biofizika **35**, 478 (1990).
[23] A. V. Panfilov and J. P. Keener, Int J. Bifurcation Chaos **3**, 445 (1993).
[24] Z. A. Jiménez, B. Marts, and O. Steinbock, Phys. Rev. Lett. **102**, 244101 (2009).
[25] X. Gao, X. Feng, M. C. Cai, B. W. Li, H. P. Ying, and H. Zhang, Phys. Rev. E **85**, 016213 (2012).
[26] H. Zhang, X. S. Ruan, B. B. Hu, and Q. Ouyang, Phys. Rev. E **70**, 016212 (2004).
[27] S. Sridhar, S. Sinha, and A. V. Panfilov, Phys. Rev. E **82**, 051908 (2010).
[28] L. Xu, Z. Qu, and Z. Di, Phys. Rev. E **79**, 036212 (2009).
[29] K. H. ten Tusscher and A. V. Panfilov, Multiscale. Model. Simul. **3**, 265 (2005).
[30] K. H. W. J. ten Tusscher and A. V. Panfilov, Phys. Rev. E **68**, 062902 (2003).
[31] I. Sendiña-Nadal, D. Roncaglia, D. Vives, V. Pérez-Muñuzuri, M. Gómez-Gesteira, V. Pérez-Villar, J. Echave, J. Casademunt, L. Ramírez-Pisicina, and F. Saqués, Phys. Rev. E **58**, R1183 (1998).
[32] P. Kuklik, L. Szumowski, P. Sanders, and J. J. Zebrowski, Comp. Bio. Med. **40**, 775 (2010).
[33] K. Agladze, M. W. Kay, V. Krinsky, and N. Sarvazyan, Am. J. Physiol. Heart Circ. Physiol **293**, H503 (2007).
[34] G. Gottwald, A. Pumir, and V. Krinsky, Chaos **11**, 487 (2001).
[35] H. Zhang, Z. Cao, N. J. Wu, H. P. Ying, and G. Hu, Phys. Rev. Lett. **94**, 188301 (2005).
[36] G. Y. Yuan, G. R. Wang, and S. G. Chen, Europhys. Lett. **72**, 908 (2005).
[37] H. Sakaguchi and T. Fujimoto, Phys. Rev. E **67**, 067202 (2003).
[38] P. Y. Wang and P. Xie, Phys. Rev. E **61**, 5120 (2000).
[39] M. Kim, M. Bertram, M. Pollmann, A. von Oertzen, A. S. Mikhailov, H. H. Rotermund, and G. Ertl, Science **292**, 1357 (2001).
[40] G. Y. Yuan, S. G. Chen, and S. P. Yang, Eur. Phys. J. B **58**, 331 (2007).
[41] M. Tanaka, A. Isomura, M. Hörning, H. Kitahata, K. Agladze, and K. Yoshikawa, Chaos **19**, 043114 (2009).
[42] A. Isomura, M. Hörning, K. Agladze, and K. Yoshikawa, Phys. Rev. E **78**, 066216 (2008).
[43] M. Hörning, A. Isomura, K. Agladze, and K. Yoshikawa, Phys. Rev. E **79**, 026218 (2009).
[44] C. Cherubini, S. Filippi, and A. Gizzi, Phys. Rev. E **85**, 031915 (2012).
[45] E. Ávalos, P. Y. Lai and C. K. Chan, Europhys. Lett. **94**, 60006 (2011).
[46] J. Cysyk and L. Tung, Biophys. J. **94**, 1533 (2008).
[47] P. Bittihn, A. Squires, G. Luther, E. Bodenschatz, V. Krinsky, U. Parlitz, and S. Luther, Philos. Trans. R. Soc. A **368**, 2221 (2010).
[48] T. K. Shajahan, B. Borek, A. Shrier, and L. Glass, Phys. Rev. E **84**, 046208 (2011).
[49] D. Olmos, Phys. Rev. E **81**, 041924 (2010).
[50] R. FitzHugh, Biophys. J. **1**, 445 (1961).
[51] M. Courtemanche, W. Skaggs, and A. T. Winfree, Physica D **41**, 173 (1990).